

Packing structure of a two-dimensional granular system through the jamming transition

Xiang Cheng^{1,2}

¹*The James Franck Institute and Department of Physics,
The University of Chicago, Chicago, Illinois 60637, USA*

²*Department of Physics, Cornell University, Ithaca, New York 14853, USA**
(Dated: October 11, 2018)

We have performed a novel experiment on granular packs composed of automatically swelling particles. By analyzing the Voronoi structure of packs going through the jamming transition, we show that the local configuration of a jamming pack is strikingly similar to that of a glass-forming liquid, both in terms of their universal area distribution and the process of defect annealing. Furthermore, we demonstrate that an unambiguous structural signature of the jamming transition can be obtained from the pair correlation functions of a pack. Our study provides insights into the structural properties of general jamming systems.

PACS numbers: 81.05.Rm, 61.43.Fs, 83.80.Fg

Nearly 300 years ago, Stephen Hales, a highly gifted English scientist and clergyman, designed a clever experiment to investigate the packing structure of spherical particles [1]. He put spherical peas into a closed jar filled with water. Absorbing the water slowly, the peas confined in the jar expanded and deformed under the enormous stress of swelling. From the shape of deformed peas, Hales deduced the structure of the initial pea pack. Though this was probably not Hales' intention, his classic experiment provides an excellent way to probe the jamming transition of a granular pack. In this paper, we report a two dimensional (2D) version of Stephen Hales' experiment. From the position of swelling particles in a cell of fixed area, we investigated the structure of a granular pack as it evolves continuously through the jamming transition.

The jamming transition and the jamming phase diagram are intriguing concepts for unifying different transitions in various systems ranging from granular matter to molecular glasses [2–8]. Many interesting features have been found in athermal granular systems near the jamming transition [3–8]. However, most of these results were obtained only in theories and simulations for ideal systems of frictionless spherical particles. It is not straightforward how such results should be extended to experimental granular systems with frictional contacts. Majmudar *et al.* found that the increasing of both the average coordination number of particles and the pressure of the system agree with the mean-field theory of frictionless particles as the jamming transition is approached [9]. However, other measurements produce different results in experiments and simulations [10–12]. For example, experiments showed that the ratio of the shear modulus to the bulk modulus of a pack, G/B , stays constant as the pressure of the system approaches zero [10, 11], which contradicts the results of simulations and theories with frictionless particles where G/B diminishes with the pressure [3, 8]. Moreover, very few experiments have di-

rectly investigated the structural signature of the jamming transition. Corwin *et al.* indirectly deduced the structural signature of the transition from the statistics of the contact forces between particles [13]. Other than granular systems, Zhang *et al.* investigated the structural signature of a colloidal system at finite temperature [14].

Here, we experimentally study the structure of a granular pack going through the jamming transition. Instead of peas, we used tapioca pearls as our granular material. Tapioca pearls are spherical particles made of starch that swell up by absorbing water. The average diameter of dry pearls is $d_0 = 3.3$ mm with the polydispersity of 8%, which prevents the system from forming large crystalline areas. A fully swelled particle can be as large as 1.7 times of its original size, which leads to almost 3 times increases in packing fraction (ϕ) of a 2D system. More importantly, the swelling of pearls is slow and uniform, and the pearls maintain their spherical shape during swelling. The polydispersity of swelled particles becomes slightly smaller than that of dry particles.

For each experiment, a single layer of pearls is laid down randomly into a square cell with the side length of $L = 54.6$ cm. The vertical height of the cell is kept at 5.454 mm using a spacer and washers, which prevents *fully* swelled pearls from buckling into two layers (Fig. 1a inset). Since the jamming transition occurs before pearls fully swell, they are not stuck between the two confining plates near the jamming point. The cell can hold over 15,000 particles at the initial packing fraction $\phi_0 \gtrsim 0.63$. A subset of the sample (about 10,000 particles) is studied in the central area of the cell to avoid any boundary effects. To allow the pearls to swell, the whole system including the cell and particles is submerged under water. Static friction between particles and the bottom plate is also reduced due to the lubrication of water. A high resolution camera is used to take an image of the sample every 20 s. Due to the slow swelling of pearls, the system is quasi-stationary at this time scale. The acquired im-

ages are then analyzed with a particle tracking algorithm [15]. The center of particles can be determined with an error of 0.1 mm (about 3% of a particle diameter). A 2D projection of images is used to obtain ϕ . More details of the experiment can be found in [16].

We initially prepared the sample in a dense but un-jammed state. As the size of particles increases, the system goes through the jamming transition and is eventually trapped inside the jammed phase. We constructed a Voronoi tessellation from the centers of particles for each image with increasing ϕ . The Voronoi cell of a particle is the polygon consisting of all points closer to the center of the particle than to centers of any other particles, which reveals local configurations of packings [1].

We first studied the area distribution of the Voronoi cells, $P(s)$, at different ϕ as the system goes through the jamming transition. We use a scaling that has been previously used in analyzing the structure of glass-forming liquids [17]. The area of each cell s is shifted by the average area of all cells $\langle s \rangle$ and then is normalized by the standard deviation σ_s , *i.e.* $\bar{s} = (s - \langle s \rangle) / \sigma_s$. The probability distribution function is then $P(\bar{s}) = \sigma_s \cdot P(s)$ (Fig. 1). The shape of normalized distributions at small ϕ depends on the initial random configuration of particles (Fig. 1a), which varies for each run. However, as ϕ increases toward the jamming point, we found that all $P(\bar{s})$ collapse into a single master curve. For clarity, the collapsed $P(\bar{s})$ is plotted separately in Fig. 1b and also in a log-linear plot in the inset of Fig. 1b. It is surprising that all the packs with ϕ ranging continuously from 0.83 up to 0.90 (which is the upper limit of our experiment due to the finite swelling potential of particles under compression) follow the same universal distribution. From the structural signature of the jamming transition which we shall show later, we know that the system jams at $\phi^* \simeq 0.84$. Hence, the universal distribution emerges only close to and after the jamming transition. It should be emphasized that the universal distribution for this large range of ϕ is non-trivial: the jammed phase of a pack is far from stationary. Though particles are confined by their neighbors, the shape of Voronoi cells is highly mobile as illustrated below. Some localized collective rearrangement of particles also exists in the jammed phase [16].

Quantitatively, we fitted the universal distribution with a shifted gamma distribution (Fig. 1b),

$$P(\bar{s}) = (\bar{s} - \bar{s}_0)^{k-1} \frac{\exp(-(\bar{s} - \bar{s}_0)/\theta)}{\Gamma(k)\theta^k}, \quad (1)$$

where θ and k are standard parameters of gamma distribution and \bar{s}_0 is a fitting parameter due to the shift in the s axis. The same distribution has been suggested before in [18, 19]. We also compare the gamma distribution with a Gaussian distribution (Fig. 1b), and find that due to the asymmetric shape of the distribution, the gamma distribution gives a better description of our data.

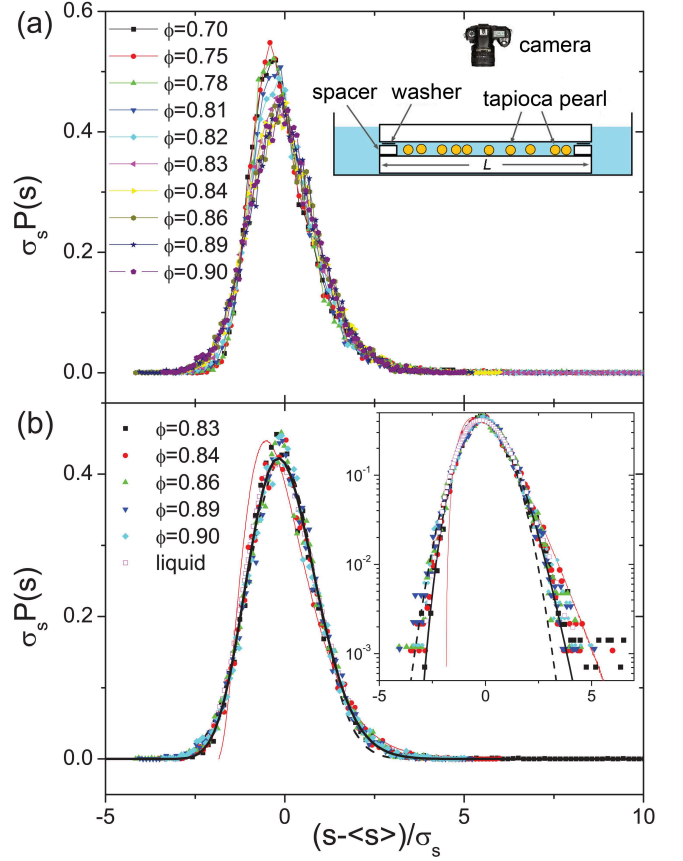


FIG. 1: Distribution of Voronoi cell areas, shifted by the average area and scaled by its standard deviation. (a) Distribution for a pack with ϕ increasing from 0.70 to 0.90. Upper right inset shows a schematic of the experimental setup. The spacer and washers keep the particles in one layer. The washers allow water to flow in and out of the otherwise closed cell. (b) The collapse of the distributions near and after the jamming transition. The universal distribution of Voronoi structure of the glass-forming liquids (empty magenta squares) is taken from [17]. The thick black line is the gamma distribution with $k = 30$ and $\theta = 0.175$. The black dashed line is a Gaussian fit. The thin red line is the distribution of Voronoi structure of random points. The inset is the log-linear plot of the same data.

Disorder and geometric constraint are two salient features of the jamming transition and the basic organizing themes underlying the jamming phase diagram. Both of them are essential in determining the shape of the universal distribution, which can be seen as following. First, it is evident that for an ordered structure the area distribution of Voronoi cells has zero variance and therefore should be a delta function (or delta functions). Second, we compare the distribution of our jamming system with that of totally random points without any geometric constraint due to particle size (Fig. 1b). For random points, the peak of the distribution shifts to the left and the distribution has longer tail toward the right.

It is known that the Voronoi structure of glass-forming liquids also follows a universal distribution at different temperatures (T) ranging from liquid states to supercooled states [17]. Even more striking, the universal distribution of the Voronoi structure of glass-forming liquids is *quantitatively* similar to the universal distribution of our 2D jamming granular system (Fig. 1b). It is likely that near the glass transition the interaction between molecules of a supercooled liquid is dominated by its strong repulsive potential, therefore, like the athermal granular system, the geometric constraint of the molecules determines the local configurations and its distribution. In addition, it is noted that deep inside the jammed phase the area distribution is invariant, which is consistent with previous study of the Voronoi structure of static granular packs at several discrete ϕ [18]. Here, we show the invariant distribution with ϕ varying continuously and uniformly in a larger range. The universal distributions of Voronoi structure in glass-forming liquids at different T and in a granular system going through the jamming transition at different ϕ corroborate the concept of the jamming phase diagram [2].

We also investigate the shape of Voronoi cells. In 2D, the geometric Euler constraint implies that average number of edges of a cell should be 6 [1, 20]. Cells with the number of edges other than 6 are usually referred to as “defects” [20–22]. We count the fractions of pentagons, hexagons and heptagons in the system (f_5, f_6 and f_7) as it goes through the jamming transition. As shown in Fig. 2, f_6 increases while f_5 and f_7 decrease: with increasing ϕ , a pentagon-heptagon pair can anneal to two hexagons. It is interesting that the annealing process continues even at ϕ clearly above the jamming point. The shape of the Voronoi cells is highly mobile due to tiny deformations of particles inside the jammed phase. Nevertheless, the annealing slows down deep inside the jammed phase and eventually stops. Due to the disordered nature of the jammed phase, a finite amount of the pentagon-heptagon pairs persist [20].

It has been proposed that the glass transition of binary-mixture molecular liquids can be characterized by the disappearance of certain kinds of “liquid-like” defects (heptagons enclosing small molecules and pentagons enclosing large molecules) in Voronoi tessellation [21, 22]. It is possible that in our granular system the “liquid-like” defects diminish during annealing and the remaining defects inside jammed phase are associated with “glass-like” defects. Due to the continuous distribution of the size of our particles and the difficulty to measure the accurate size of particles under water, we cannot directly verify the above scenario. However, a consistency check can be made by analyzing the average area of different types of cells. If heptagons enclosing small molecules, which should have smaller Voronoi cells in a condensed phase on average, diminish, then the average area of heptagons normalized by the total average area, should increase.

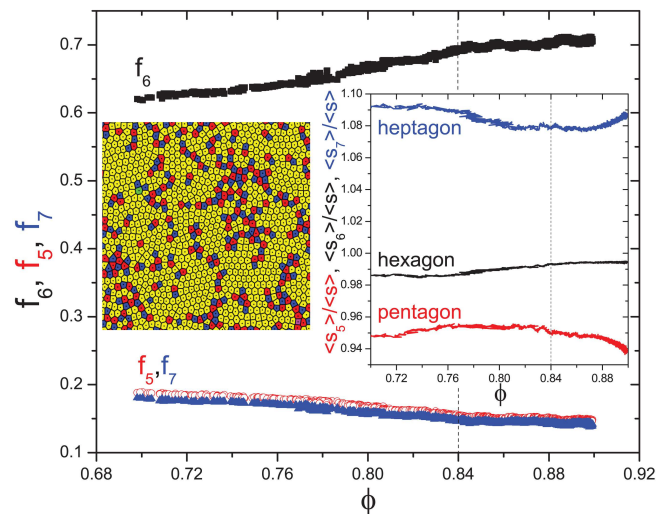


FIG. 2: Main plot: Number fraction of different type of cells with increasing ϕ . Black squares for hexagons (f_6), red circles for pentagons (f_5) and blue triangles for heptagons (f_7). Left inset: Shape of cells in Voronoi tessellation of a pack at $\phi = 0.86$. Yellow cells are hexagons; blue cells are pentagons and red cells are heptagons. There is also one octagon (green) and one square (magenta). Note that most of pentagons and heptagons join into neighboring pairs and can anneal to hexagons later. Right inset: the average area of hexagons, pentagons and heptagons over the total average area of cells. The vertical dashed lines in both plots indicate the jamming point obtained from the structural signature of the jamming transition explained in the text.

Similarly, if pentagons enclosing large molecules disappear, then the average area of pentagons over the total average area should decrease. We measured the normalized average area of pentagons, hexagons and heptagons, $\langle s_5 \rangle / \langle s \rangle$, $\langle s_6 \rangle / \langle s \rangle$ and $\langle s_7 \rangle / \langle s \rangle$, as a function of ϕ in our experiments (Fig. 2 right inset). First, we can see pentagons have smaller area on average ($\langle s_5 \rangle / \langle s \rangle < 1$) and heptagons have larger area on average ($\langle s_7 \rangle / \langle s \rangle > 1$). The trends of $\langle s_5 \rangle / \langle s \rangle$, $\langle s_6 \rangle / \langle s \rangle$ and $\langle s_7 \rangle / \langle s \rangle$ are more interesting. Before jamming the trends depend on the initial packing configuration of individual experiment, similar to the behavior of $P(\bar{s})$ before jamming. However, close to and after the jamming transition their features are robust for all experiments: $\langle s_6 \rangle / \langle s \rangle$ plateaus, but $\langle s_5 \rangle / \langle s \rangle$ clearly decreases and $\langle s_7 \rangle / \langle s \rangle$ increases. This is consistent with the behavior of glass-forming liquids [21, 22].

Before we can explore the relation between the glass transition and the jamming transition further, we need to ask a simple but important question: where does an athermal system jam? Though the jamming point of a pack can be easily identified by its mechanical properties [3], experimentally it is usually hard to acquire further information of a pack except the position of all its particles. Can we detect the jamming transition of a granular

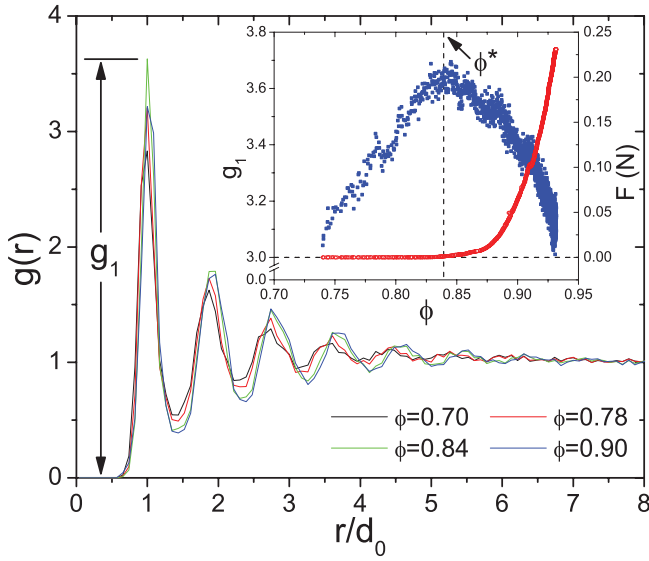


FIG. 3: Pair correlations of a pack at different ϕ . r is normalized by the original size of pearls d_0 . The height of the first peak, g_1 , is indicated. Inset: The height of the first peak $g_1(\phi)$ (blue squares) and the force measured at the boundary of the cell $F(\phi)$ (red circles). The vertical dashed line indicates the peak of $g_1(\phi)$, ϕ^* . The horizontal dashed line indicates the zero force.

pack from its structure? Despite the interesting features shown above, the Voronoi tessellation does not provide a unambiguous standard of the jamming transition. Both the area distribution and the annealing of defects show only quantitative changes before and after the transition. We shall show next that, for a pack of granular particles with purely repulsive interactions, its pair correlation provides a structural signature of the jamming transition.

We plot the pair correlation functions, $g(r)$, of a pack at different ϕ through the jamming transition (Fig. 3). At each ϕ , $g(r)$ has an oscillating shape, typical for amorphous packs of spherical particles. Peaks in $g(r)$ indicate the layering structure in the pack, the positions of which shift to larger r as ϕ increases due to the enlargement of particles. A structural signature of the jamming transition can be obtained by measuring g_1 , the height of the first peak of $g(r)$. $g_1(\phi)$ shows a non-monotonic behavior with a peak at $\phi^* = 0.84 \pm 0.02$ (Fig. 3 inset). We also measured the force applied by the pack on the boundary of the cell (Fig. 3 inset). The jamming point of the system is marked by the emergence of a non-zero force on the boundary, which is coincident with the peak of $g_1(\phi)$. Hence, $g_1(\phi)$ provides a clear structural signature of the jamming transition and ϕ^* is the jamming point.

The non-monotonic behavior of $g_1(\phi)$ can be seen as the vestige of the structural singularity uncovered in the jamming transition of monodisperse frictionless particles [4]. As a system evolves from unjammed state toward

ϕ^* , particles are pushed closer to each other. The distribution of the distance between neighboring particles becomes narrower and g_1 therefore increases. For monodisperse frictionless particles, due to the finite range purely repulsive interaction, at the jamming point the distances between contact particles are all exactly one particle diameter. Hence, g_1 , representing the probability to find a neighboring particle at a fixed distance, diverges. However, it should be noted that for a system consisting of particles with attractive interactions the onset of complete connectivity of all particles and the rigidity of the pack need not occur at the same packing fraction. Above ϕ^* , due to the disordered nature of the pack, particles will experience different compression and deform differently depending on their local environment. The distances between contact particles spread out again. Quantitatively, $g_1 \cdot w \sim z$ above jamming, where w is the left-hand width of the first peak of $g(r)$ and z is the average coordination number of particles [4]. Since z increases slowly, it can be treated approximately as a constant near ϕ^* . Hence, as w increases from zero above ϕ^* , g_1 decreases. Apparently, the polydispersity of our particles depresses the divergence of g_1 . Even at ϕ^* , the distribution of the distances between contact particles still has a finite width. Nevertheless, a non-monotonic peak is preserved as a vestige of the singularity. A simple estimation can be made on $g_1(\phi^*)$ with polydisperse particles. Due to the difficulty to accurately measure the size of swelled soft particles, we estimate the polydispersity of swelled particles at ϕ^* to be around 5 to 8 percent, which is slightly smaller than that of dry particles. If we assume that there is no correlation between the radius of one particle and the radius of its neighbors, w should be roughly equal to the polydispersity of particles, *i.e.* $w = 5\% \sim 8\%$ at ϕ^* . Using the relation $g_1(w)$ obtained from the simulations (Fig. 2 of Ref.[4]), we found that $2.8 < g_1(\phi^*) < 4.5$, which is consistent with our measurement (Fig. 3 inset). A similar thermal vestige of the structural singularity has also been observed in a colloidal system of finite T [14], where the structural singularity is depressed by the thermal motion instead.

By analyzing the Voronoi tessellation and the pair correlation functions of a granular pack with increasing ϕ , we have investigated the packing structures of the jamming transition. We have shown that the local configurations of a jamming granular pack are similar to those of glass-forming liquids, thereby demonstrating the analogy between the jamming transition and the glass transition in the spirit of the jamming phase diagram. Further study of the local structure of other jamming systems, such as glassy colloidal suspensions or jammed foams, may shed more light on the universal properties of the jamming structure illustrated here. Moreover, we have shown that a structural signature of the jamming transition can be obtained from the first peak of pair correlation functions. Our study shows that, despite the

presence of realistic conditions such as frictional contacts and non-perfect spherical particle shapes, the structural signature observed in the ideal jamming system still persists in actual experiments.

The author thanks S. Nagel and H. Jaeger for their support and guidance. I am grateful to E. Brown, N. Keim, J. Royer, N. Xu and L.-N. Zou for their help with the experiments and fruitful discussions. I also thank L. Ristroph and S. Gerbode for comments on the manuscript. This work was supported by the NSF MR-SEC program under DMR-0820054, by the Keck Initiative for Ultrafast Imaging at the University of Chicago and by the DOE under DE-FG02-03ER46088.

* Electronic address: xc92@cornell.edu

- [1] T. Aste and D. Weaire, *The Pursuit of Perfect Packing*, Taylor and Francis, New York, ed. 2, 2008.
- [2] A. J. Liu and S. R. Nagel, *Nature*, 1998, **396**, 21-22.
- [3] C. S. O'Hern, L. E. Silbert, A. J. Liu and S. R. Nagel, *Phys. Rev. E*, 2003, **68**, 011306.
- [4] L. E. Silbert, A. J. Liu and S. R. Nagel, *Phys. Rev. E*, 2006, **73**, 041304.
- [5] W. G. Ellenbroek, E. Somfai, M. van Hecke and W. van Saarloos, *Phys. Rev. Lett.*, 2006, **97**, 258001.
- [6] P. Olsson and S. Teitel, *Phys. Rev. Lett.*, 2007, **99**, 178001.
- [7] S. Henkes and B. Chakraborty, *Phys. Rev. Lett.*, 2005, **95**, 198002.
- [8] M. Wyart, L. E. Silbert, S. R. Nagel and T. A. Witten, *Phys. Rev. E*, 2005, **72**, 051306.
- [9] T. S. Majmudar, M. Sperl, S. Luding and R. P. Behringer, *Phys. Rev. Lett.*, 2007, **98**, 058001.
- [10] X. Jacob, V. Aleshin, V. Tournat, P. Leclaire, W. Lauriks and V. E. Gusev, *Phys. Rev. Lett.*, 2008, **100**, 158003.
- [11] L. Bonneau, B. Andreotti and E. Clément, *Phys. Rev. Lett.*, 2008, **101**, 118001.
- [12] M. M. Bandi, M. K. Rivera, F. Krzakala and R. E. Ecke, 2009, arXiv:0910.3008.
- [13] E. I. Corwin, H. M. Jaeger and S. R. Nagel, *Nature*, 2005, **435**, 1075-1078.
- [14] Z. Zhang *et al.*, *Nature*, 2009, **459**, 230-233.
- [15] J. C. Crocker and D. G. Grier, *J. Colloid Interface Sci.*, 1996, **179**, 298-310.
- [16] X. Cheng, *Phys. Rev. E*, 2010, **81**, 031301.
- [17] F. W. Starr, S. Sastry, J. F. Douglas and S. C. Glotzer, *Phys. Rev. Lett.*, 2002, **89**, 125501.
- [18] T. Aste, T. Di Matteo, M. Saadatfar, T. J. Senden, M. Schröter and H. L. Swinney, *Europhys. Lett.*, 2007, **79**, 24003.
- [19] V. S. Kumar and V. Kumaran, *J. Chem. Phys.*, 2005, **123**, 114501.
- [20] D. N. Perera and P. Harrowell, *Phys. Rev. E*, 1999, **59**, 5721-5743.
- [21] E. Aharonov, E. Bouchbinder, H. G. E. Hentschel, V. Ilyin, N. Makedonska, I. Procaccia and N. Schupper, *Europhys. Lett.*, 2007, **77**, 56002.
- [22] H. G. E. Hentschel, V. Ilyin, N. Makedonska, I. Procaccia and N. Schupper, *Phys. Rev. E*, 2007, **75**, 050404.